

# BENCHMARKING FOR THE NUMERICAL PREDICTION OF SOUND TRANSMISSION THROUGH SLITS, PLATES AND SHELLS

R. PISCOYA, N. GORENFLO, M. OCHMANN

*Beuth Hochschule für Technik Berlin - University of Applied Sciences, Germany  
piscoya@beuth-hochschule.de, gorenflo@beuth-hochschule.de,  
ochmann@beuth-hochschule.de*

## **Abstract**

*In the present paper, a numerical approach for the prediction of the sound transmission through slits, plates and shells is implemented and its accuracy is tested solving some benchmark problems. The method is based on the Boundary Element Method (BEM) which solves an integral equation at the slit or at the surface of the structure to determine the sound propagation. In the case that the slit or flat plate lies on an infinite rigid baffle, the integral equation simplifies to a Rayleigh integral. The benchmark problems presented here are i) a 2D-slit, ii) a simply supported baffled plate and iii) a spherical elastic shell.*

## **Introduction**

The transmission of sound through openings and plate-like structures is important in building acoustics to characterize noise pollution and sound insulation between adjacent rooms. The transmission loss of simple structures can be estimated by simplified expressions but when dealing with complex structures, which is mostly the case for practical applications, numerical methods have to be used. The BEM is a very useful tool when the sound propagation is studied in an unbounded medium, but it can be also successfully employed for the sound transmission in buildings as an alternative to other methods like the FEM or modal decomposition that are available for interior problems.

In the following sections, the application of the BEM to three transmission problems is presented. The numerical results are compared with other known solutions to investigate the accuracy and applicability of the numerical approach.

## **Transmission through a slit**

We consider the case of a plane wave having an obliquely incidence on an infinite rigid plane with a slit. For simplicity, the baffle is perpendicular to the  $Z$  axis and located at  $z=0$ .

The media below and above the baffle are not necessarily the same. The surface of the slit is denoted by  $S$ .

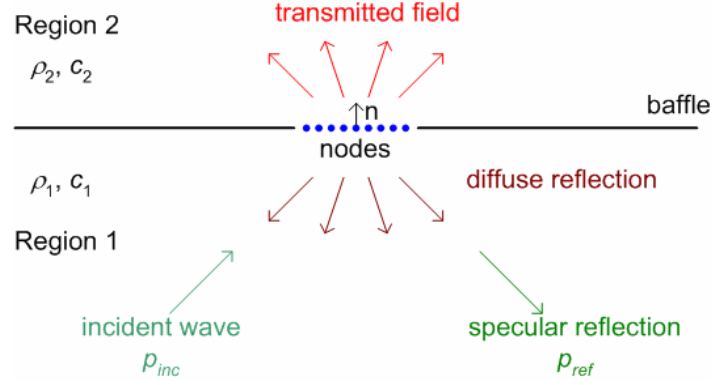


Fig. 1: Transmission of a plane wave through a slit

The sound field at both sides of the infinite baffle is given by the expressions

$$\begin{aligned} p_1 &= p_{inc} + p_{ref} + \int_S \frac{\partial p_1^S}{\partial n} g_{H,1} dS && \text{in Region 1} \\ p_2 &= - \int_S \frac{\partial p_2^S}{\partial n} g_{H,2} dS && \text{in Region 2} \end{aligned} \quad (1)$$

where  $p_{ref}$  is the sound wave reflected specularly at the baffle without the slit and  $g_{H1}$  and  $g_{H2}$  are the Green's functions in each medium with vanishing normal derivative at the baffle

$$\frac{\partial g_{H,1}}{\partial n} = \frac{\partial g_{H,2}}{\partial n} = 0. \quad (2)$$

Expressions (1) are valid for the two- and three-dimensional case, but the Green's functions are different

$$g_H = \begin{cases} \frac{1}{2j} H_0^{(2)}(k|\bar{x} - \bar{y}|) & \text{in 2D} \\ \frac{e^{-jk|\bar{x} - \bar{y}|}}{2\pi|\bar{x} - \bar{y}|} & \text{in 3D} \end{cases} \quad (3)$$

In the slit, the sound pressure and the normal particle velocity must be continuous. These conditions lead to the relation:

$$\int_S j\omega v_n^S (\rho_1 g_{H1} + \rho_2 g_{H2}) dS = p_{inc}|_{z=0} + p_{ref}|_{z=0} \quad (4)$$

For the plane wave,  $p_{ref}|_{z=0} = p_{inc}|_{z=0}$  and if the same medium is assumed at both sides of the baffle,  $\frac{\partial p_1^S}{\partial n} = \frac{\partial p_2^S}{\partial n} = \frac{\partial p^S}{\partial n}$  and Eq. (4) is simplified to

$$- \int_S \frac{\partial p^S}{\partial n} g_H dS = p_{inc}|_{z=0} \quad (5)$$

Eq. (5) together with Eq. (1) shows that the sound pressure in the slit is the same as if there were no baffle at all, which is a somewhat surprising result.

For the numerical calculations, the area of the slit is discretized in a finite number of elements ( $N_e$ ) and nodes ( $N_n$ ). Considering constant elements, i.e. all quantities are constant over an element, the surface integral can be expressed as a sum over all elements. A system

of equations is built and the normal derivative of the sound pressure in each element can be obtained. The sound field at every point of the space can be calculated once  $\partial p / \partial n$  is known. As a well known practical rule of thumb points out, at least six points per wavelength are needed in order to obtain good accuracy.

The results obtained by the numerical approach can be validated by comparing them with an analytical approach for the case of a two-dimensional slit of length 2 (see [1]).

The integral equation in 2D to be solved has  $\partial p / \partial n$  as unknown variable

$$\int_{-1}^1 \phi(x') H_0^{(2)}(k|x-x'|) dx' = f(x) , \quad (6)$$

with  $\phi = \partial p / \partial n$  and  $f = -j2p|_{z=0}$ . According to [1],  $\phi$  can be expanded in a series of even or odd functions depending on whether  $f$  is even or odd.

$$\phi(x) = \sum_n c_n \begin{Bmatrix} \phi_n^{(e)}(x) \\ \phi_n^{(o)}(x) \end{Bmatrix} \quad (7)$$

with

$$\begin{aligned} \phi_{2j+1}^{(e)}(x) &= x^{2j} \cos(kx) \quad \text{and} \quad \phi_{2j+2}^{(e)}(x) = x^{2j+1} \sin(kx) \quad \text{or} \\ \phi_{2j+1}^{(o)}(x) &= x^{2j} \sin(kx) \quad \text{and} \quad \phi_{2j+2}^{(o)}(x) = x^{2j+1} \cos(kx) . \end{aligned}$$

Inserting Eq. (7) into (6) yields,

$$\sum_n c_n \int_{-1}^1 \begin{Bmatrix} \phi_n^{(e)}(x') \\ \phi_n^{(o)}(x') \end{Bmatrix} H_0^{(2)}(k|x-x'|) dx' = f(x) . \quad (8)$$

The integrals in (8) can be computed explicitly

$$\int_{-1}^1 \phi_n^{(e)}(x') H_0^{(2)}(k|x-x'|) dx' = f_n^{(e)}(x) , \quad (9)$$

$$\int_{-1}^1 \phi_n^{(o)}(x') H_0^{(2)}(k|x-x'|) dx' = f_n^{(o)}(x) \quad (10)$$

with

$$\begin{aligned} f_n^{(e)}(x) &= p_n^{(1)}(x) H_0^{(2)}(k|x+1|) + p_n^{(1)}(-x) H_0^{(2)}(k|x-1|) + \\ &\quad q_n^{(1)}(x) \operatorname{sgn}(x+1) H_1^{(2)}(k|x+1|) - q_n^{(1)}(-x) \operatorname{sgn}(x-1) H_1^{(2)}(k|x-1|) , \\ f_n^{(o)}(x) &= p_n^{(2)}(x) H_0^{(2)}(k|x+1|) - p_n^{(2)}(-x) H_0^{(2)}(k|x-1|) + \\ &\quad q_n^{(2)}(x) \operatorname{sgn}(x+1) H_1^{(2)}(k|x+1|) + q_n^{(2)}(-x) \operatorname{sgn}(x-1) H_1^{(2)}(k|x-1|) , \end{aligned}$$

where  $p_n^{(1)}$ ,  $q_n^{(1)}$ ,  $p_n^{(2)}$  and  $q_n^{(2)}$  are polynomials. One of the polynomials  $p_n^{(1)}$  and  $q_n^{(1)}$  is of degree  $n$  and the other of degree not greater than  $n$ . The same holds for  $p_n^{(2)}$  and  $q_n^{(2)}$ . The polynomial coefficients can be computed by recursion formulas.

Replacing (9) and (10) in (8) yields

$$\sum_n c_n \begin{Bmatrix} f_n^{(e)}(x) \\ f_n^{(o)}(x) \end{Bmatrix} = f(x) . \quad (11)$$

For a practical application, the series is truncated after  $N$  terms. The coefficients  $c_n$  are computed by solving a system of equations obtained by multiplying (11) with  $x^{2j} \cos(kx)$  if  $f$  is even or  $x^{2j+1} \cos(kx)$  if  $f$  is odd and integrating over the interval  $[-1,1]$ ,

$$\sum_{n=1}^N c_n \begin{Bmatrix} \int_{-1}^1 x^{2j} \cos(kx) f_n^{(e)}(x) dx \\ \int_{-1}^1 x^{2j+1} \cos(kx) f_n^{(o)}(x) dx \end{Bmatrix} = \int_{-1}^1 \begin{Bmatrix} x^{2j} \\ x^{2j+1} \end{Bmatrix} \cos(kx) f(x) dx , \quad j=0, 1, \dots, N-1. \quad (12)$$

If  $f$  is neither even nor odd, one can solve two linear systems, one for the even part of  $f$ , that is  $[f(x) + f(-x)]/2$ , and one for the odd part  $[f(x) - f(-x)]/2$ .

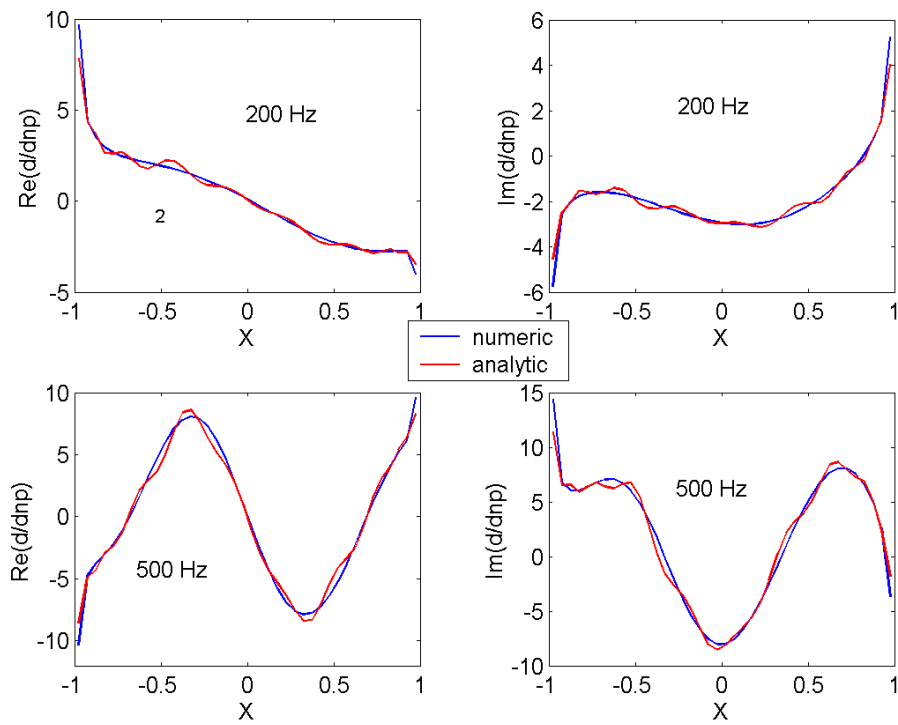


Fig. 2: Normal derivative of the pressure in the slit at 200 Hz and 500 Hz, left: real part; right: imaginary part.

The agreement between the numerical and the analytical results is very good as shown in Fig. 2. The number of terms considered in the expansion (7) was ten ( $N=10$ ) and it proved to be enough. The number of functions needed increases with the frequency as well as the number of nodes and elements for the numerical approach. The small differences in the pressure derivative in the slit do not affect the far field as can be seen in Fig. 3. The incidence angle of the wave is the same angle at which the transmitted wave has its maximum.

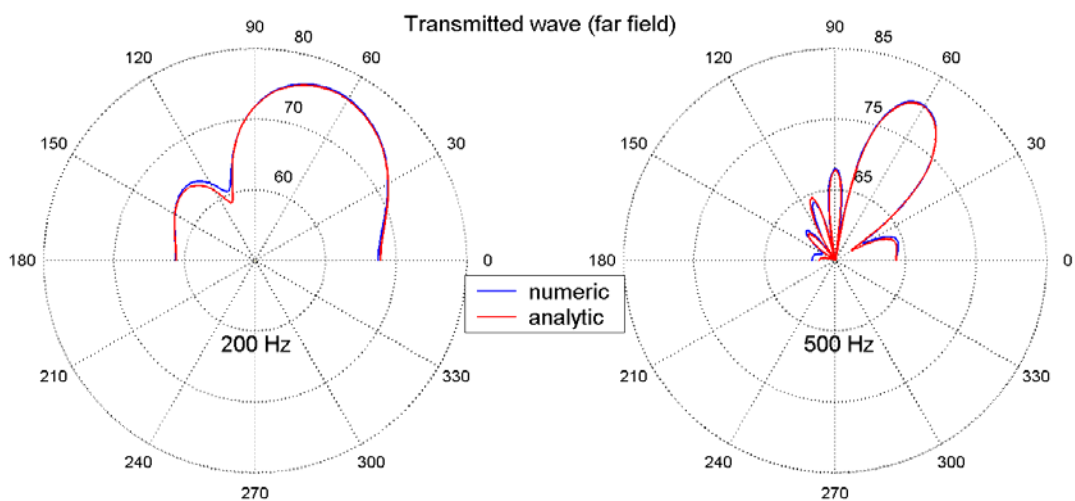


Fig. 3: Directivity of the transmitted wave at 200 Hz and 500 Hz.

## Transmission through a baffled plate

We now cover the opening on the baffle with a thin flat plate. The sound field at both sides of the baffle is given by the same expressions (1). For this problem, we consider only the normal displacement of the plate. The normal displacement of the fluid that touches the plate is the same as the normal displacement of the plate  $u_f^S = u$ . Since  $\partial p / \partial n = \rho \omega^2 u_f$ , we write Eqs. (1) as

$$\begin{aligned} p_1 &= p_{inc} + p_{ref} + \rho_1 \omega^2 \int_S u g_{H,1} dS & \text{in Region 1} \\ p_2 &= -\rho_2 \omega^2 \int_S u g_{H,2} dS & \text{in Region 2} \end{aligned} \quad (13)$$

The plate is discretized in elements ( $N_e$ ) and nodes ( $N_n$ ). The displacement of the center of the element satisfies the matrix equation

$$(K - \omega^2 M)u = F^m, \quad (14)$$

where  $M$  is the mass matrix,  $K$  is the stiffness matrix and  $F^m$  is the vector of external loads defined as

$$F_i^m = (p_{i1}^S - p_{i2}^S)A_i, \quad (15)$$

assuming again constant elements.

Combining Eqs. (13)-(15), the coupled system of equations for  $u$ ,  $p_1^S$  and  $p_2^S$  is given by

$$\begin{bmatrix} K - \omega^2 M & -A & A \\ -\rho_1 \omega^2 G_{H,1} & 1 & 0 \\ \rho_2 \omega^2 G_{H,2} & 0 & 1 \end{bmatrix} \begin{bmatrix} u \\ p_1^S \\ p_2^S \end{bmatrix} = \begin{bmatrix} 0 \\ p_{inc}^S + p_{ref}^S \\ 0 \end{bmatrix}, \quad (16)$$

where  $A$  is the matrix containing the surface of the elements.

The system of Eqs. (16) can be reduced to a system of equations for  $u$  only:

$$((K - \omega^2 M) - \rho_1 \omega^2 A G_{H,1} - \rho_2 \omega^2 A G_{H,2})u = A(p_{inc}^S + p_{ref}^S) \quad (17)$$

and the other variables are obtained directly from  $u$  using the relations

$$p_1^S = p_{inc}^S + p_{ref}^S + \rho_1 \omega^2 G_{H,1} u, \quad p_2^S = -\rho_2 \omega^2 G_{H,2} u. \quad (18)$$

The system of equations in (17) can be very large if the discretization of the object is very fine, but it can be reduced if the displacement vector is expressed as a linear combination of structural modes in vacuum:

$$u(\vec{x}) = \sum_i \alpha_i \phi_i(\vec{x}) \rightarrow u = \phi \alpha. \quad (19)$$

The coefficients  $\alpha_i$  are called participation factors. Normally they decrease with the order of the modes, so the number of modes needed to achieve results within a certain error margin should be much lower than the number of nodes. Assuming there is no damping in the structure, the modes are orthogonal and satisfy the equation

$$(K - \omega_i M)\phi_i = 0 \quad \text{with} \quad \phi_j^T K \phi_i = \phi_j^T M \phi_i = 0, \quad i \neq j. \quad (20)$$

Replacing Eq. (19) in (17) and multiplying both sides by  $\phi^T$  we obtain

$$((\tilde{K} - \omega^2 \tilde{M}) - \rho_1 \omega^2 Q_1 - \rho_2 \omega^2 Q_2)\alpha = b, \quad (21)$$

with

$$\begin{aligned} \tilde{K} &= \phi^T K \phi, & \tilde{M} &= \phi^T M \phi \\ Q_1 &= \phi^T A G_{H,1} \phi, & Q_2 &= \phi^T A G_{H,2} \phi, & b &= \phi^T A (p_{inc}^S + p_{ref}^S). \end{aligned}$$

The matrix to be inverted in Eq. (21) is a  $n \times n$  square matrix with  $n < N_e$ ,  $n$ =number of modes. Because of the orthogonality of the eigenvectors and the symmetry of  $K$  and  $M$ , the matrices  $\tilde{K}$  and  $\tilde{M}$  are diagonal.

The transmission factor ( $\tau$ ) of the baffled plate is given by the expression

$$\tau = \frac{\text{transmitted power } (W_{tr})}{\text{incident power } (W_{inc})},$$

with

$$W_{tr} = \frac{1}{2} \int_S \text{Re}(p_2^S(-j\omega u^*)) dS, \quad W_{inc} = \frac{1}{2} \int_S \text{Re}(p_{inc}(v_{n,inc}^S)^*) dS.$$

To evaluate the accuracy of the results provided by this method, a comparison of the TL of a simply supported plate is made with the results obtained with a generalized model developed by Woodcock and Nicolas [2]. In their approach, the displacement of the plate is expanded in a basis of polynomials

$$u(x, y) = \sum_{n,m} c_{nm} \left(\frac{2x}{a}\right)^n \left(\frac{2y}{b}\right)^m,$$

where  $a$  and  $b$  are the dimensions of the plate, and general boundary conditions of elastic type are imposed along the contour through translational and rotational springs. The mass and stiffness matrices are obtained via a variational formulation and the eigenmodes and eigenfrequencies can be obtained solving an eigenvalue equation for the coefficients  $c_{nm}$  similar to Eq. (20). For the transmission problem, the following matrix equation for the coefficients  $c_{nm}$  is solved

$$\left[ K_{pqnm} - \omega^2 M_{pqnm} + j\omega(Z_{pqnm}^{(1)} + Z_{pqnm}^{(2)}) \right] c_{nm} = P_{pq}^{BP}, \quad (22)$$

with

$$P_{pq}^{BP} = \int_{-a/2}^{a/2} \int_{-b/2}^{b/2} 2p_{inc}(x, y, 0) \left(\frac{2x}{a}\right)^p \left(\frac{2y}{b}\right)^q dx dy, \quad (23)$$

$$Z_{pqnm}^{(1,2)} = j\rho_{1,2}\omega \int_{-a/2}^{a/2} \int_{-b/2}^{b/2} g_{1,2}(x, y, x', y') \left(\frac{2x}{a}\right)^p \left(\frac{2y}{b}\right)^q \left(\frac{2x'}{a}\right)^n \left(\frac{2y'}{b}\right)^m dx' dy' dx dy. \quad (24)$$

The vector  $P_{pq}^{BP}$  and the real part of the matrix  $Z_{pqnm}^{(1,2)}$  can be computed analytically in a direct way, while the imaginary part of  $Z_{pqnm}^{(1,2)}$  is much more complicated. According to [2], for light media,  $\text{Im}(Z_{pqnm}^{(1,2)})$  can be neglected.

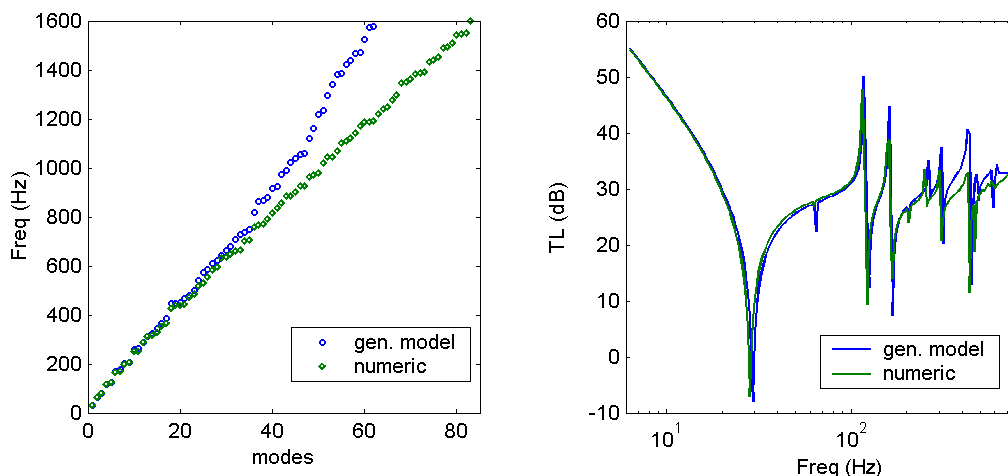


Fig. 4: Eigenfrequencies and Transmission Loss of a simply supported steel plate.

In Fig. 4, a comparison of the eigenfrequencies and the TL of the baffled steel plate obtained with the numerical approach and the generalized model is shown. The first modes agree very well up to about 400 Hz, for higher modes the differences start to increase because the high eigenfrequencies in the generalized model demand a high accuracy in the calculation of the elements of  $K$  and  $M$ . The TL curves agree well in the low frequencies and the differences become bigger beyond 400 Hz, possibly because of the differences in the eigenfrequencies and also the omission of  $\text{Im}(Z_{pqnm}^{(1,2)})$ . That term becomes more significant if the plate is light compared to the medium as can be seen in Fig. 5. In that case, neglecting  $\text{Im}(Z_{pqnm}^{(1,2)})$  provides a big error.

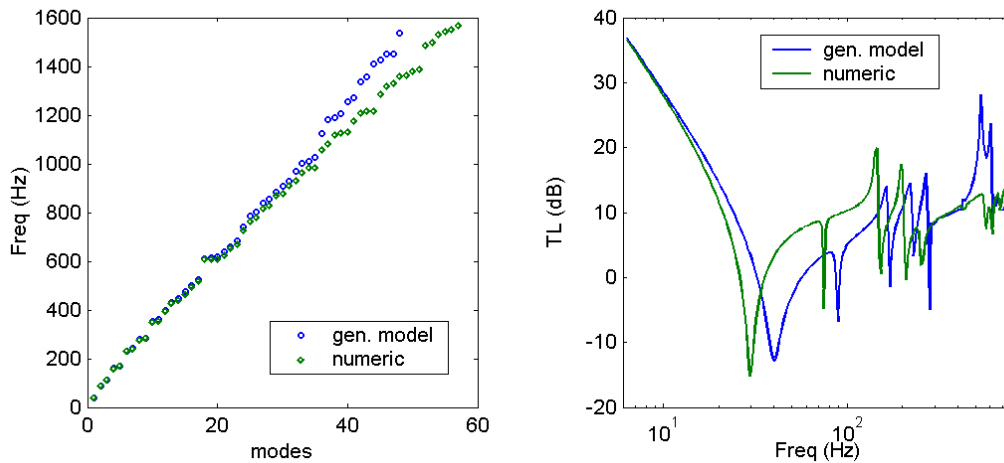


Fig. 5: Eigenfrequencies and Transmission Loss of a simply supported light plate.

### Transmission through a thin shell

We consider now a more general situation, where the incident plane wave encounters a three dimensional thin elastic body of thickness  $h$  and with arbitrary shape. The structure contains a fluid which may be different from the outside medium (Fig. 6)

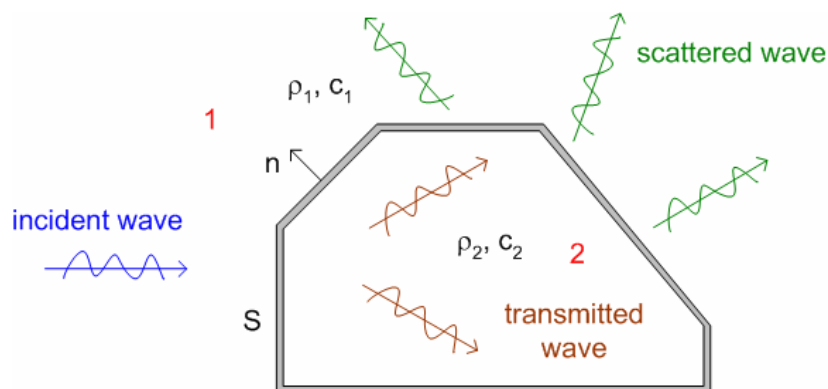


Fig. 6: Transmission of a plane wave through a thin shell.

The sound field inside and outside the body is given by the expressions

$$\begin{aligned} C_1 p_1 &= \int_S \left( p_1^S \frac{\partial g_1}{\partial n_1} - \rho_1 \omega^2 u_n g_1 \right) dS + p_{inc} \quad \text{in 1} \\ C_2 p_2 &= - \int_S \left( p_2^S \frac{\partial g_2}{\partial n_2} - \rho_2 \omega^2 u_n g_2 \right) dS \quad \text{in 2} \end{aligned} \quad (25)$$

where  $u_n$  denotes the normal component of the displacement of the structure.

Discretizing the body with constant elements, and evaluating Eq. (25) at each element we obtain the matrix expressions

$$\begin{aligned} (0.5I - H_1) p_1^S &= p_{inc}^S - \rho_1 \omega^2 G_1 u_n \quad \text{in 1} \\ (0.5I + H_2) p_2^S &= \rho_2 \omega^2 G_2 u_n \quad \text{in 2} \end{aligned} \quad (26)$$

The motion of the body is given by Eq. (14) with

$$\begin{aligned} \mathbf{u} &= [u_{x1} \ u_{y1} \ u_{z1} \ \dots \ u_{xN} \ u_{yN} \ u_{zN}]^T, \\ \mathbf{F}^m &= [F_{x1} \ F_{y1} \ F_{z1} \ \dots \ F_{xN} \ F_{yN} \ F_{zN}]^T, \end{aligned}$$

and the components of the load of the medium at the  $i$ -th element are defined as in [3]

$$F_{xi} = -(p_{1i}^S - p_{2i}^S) n_{xi} A_i, \quad F_{yi} = -(p_{1i}^S - p_{2i}^S) n_{yi} A_i, \quad F_{zi} = -(p_{1i}^S - p_{2i}^S) n_{zi} A_i. \quad (27)$$

Combining Eqs. (26), (27) and (14), a matrix equation for  $\mathbf{u}$  can be deduced:

$$\left( (K - \omega^2 M) - \rho_1 \omega^2 \tilde{N}^T (WS^{(1)}) \tilde{N} - \rho_2 \omega^2 \tilde{N}^T (WS^{(2)}) \tilde{N} \right) \mathbf{u} = -\tilde{N}^T (PS), \quad (28)$$

with the following matrices

$$\tilde{N} = \begin{pmatrix} n_1 & 0 & \dots & 0 \\ 0 & n_2 & 0 & \vdots \\ \vdots & 0 & \ddots & 0 \\ 0 & \dots & 0 & n_E \end{pmatrix}, \quad n_i = [n_{xi} \ n_{yi} \ n_{zi}]^T, \quad (29)$$

$$WS^{(k)} = \begin{pmatrix} W_{11}^{(k)} \Delta S_1 & W_{12}^{(k)} \Delta S_1 & \dots & W_{1N}^{(k)} \Delta S_1 \\ W_{21}^{(k)} \Delta S_2 & W_{22}^{(k)} \Delta S_2 & \dots & W_{2N}^{(k)} \Delta S_2 \\ \vdots & \vdots & \ddots & \vdots \\ W_{N1}^{(k)} \Delta S_N & W_{N2}^{(k)} \Delta S_N & \dots & W_{NN}^{(k)} \Delta S_N \end{pmatrix}, \quad PS = \begin{pmatrix} Hp_{i1} \Delta S_1 \\ Hp_{i2} \Delta S_2 \\ \vdots \\ Hp_{iN} \Delta S_N \end{pmatrix}, \quad (30)$$

$$W^{(1)} = (0.5I - H_1)^{-1} G_1, \quad W^{(2)} = (0.5I + H_2)^{-1} G_2, \quad Hp = (0.5I - H_1)^{-1} p_{inc}. \quad (31)$$

If the displacement is expanded in the eigenvalues in vacuum as in Eq. (19), the equation for the coefficients  $\alpha$  is written as

$$\left\{ \phi^T (K - \omega^2 M) \phi + j\omega(Z_1 + Z_2) \right\} \alpha = (\tilde{N}\phi)^T (PS), \quad (32)$$

with

$$Z_1 = j\omega\rho_1 (\tilde{N}\phi)^T (WS^{(1)}) \tilde{N}\phi, \quad (33)$$

$$Z_2 = j\omega\rho_2 (\tilde{N}\phi)^T (WS^{(2)}) \tilde{N}\phi. \quad (34)$$

In order to evaluate the results of the numerical approach, we consider a spherical thin shell of radius  $a$  as the structure, since for this case there is an analytical solution. Following the Kirchhoff-Love theory, if no torsional vibrations are considered ( $u_\phi = 0$ ), the normal and tangential displacement ( $u_r$  and  $u_\theta$ ) of the middle surface is given by the following set of equations [4]

$$L_{11} u_\theta + L_{13} u_r = \frac{\rho h}{Y} \frac{\partial^2 u_\theta}{\partial t^2}, \quad Y = \frac{Eh}{1-\nu^2}, \quad (35.a)$$



$$L_{31}u_\theta + L_{33}u_r = \frac{1}{Y} \left( -\rho h \frac{\partial^2 u_r}{\partial t^2} + p_{ext} \right), \quad (35.b)$$

$$L_{11} = \frac{1+\beta^2}{a^2} \left( \frac{\partial^2}{\partial \theta^2} + \cot \theta \frac{\partial}{\partial \theta} - \nu - \cot^2 \theta \right), \quad (35.c)$$

$$L_{13} = \frac{-\beta^2}{a^2} \left( \frac{\partial^3}{\partial \theta^3} + \cot \theta \frac{\partial^2}{\partial \theta^2} - (\nu + \cot^2 \theta) \frac{\partial}{\partial \theta} \right) + \frac{1+\nu}{a^2} \frac{\partial}{\partial \theta}, \quad (35.d)$$

$$L_{31} = \frac{-\beta^2}{a^2} \left( \frac{\partial^3}{\partial \theta^3} + 2 \cot \theta \frac{\partial^2}{\partial \theta^2} - (1+\nu + \cot^2 \theta) \frac{\partial}{\partial \theta} + \cot \theta \left( 1-\nu + \frac{1}{\sin^2 \theta} \right) \right) + \frac{1+\nu}{a^2} \left( \frac{\partial}{\partial \theta} + \cot \theta \right), \quad (35.e)$$

$$L_{33} = \beta^2 a^2 \left( \nabla_\theta^2 \nabla_\theta^2 + \frac{1-\nu}{a^2} \nabla_\theta^2 \right) + \frac{2(1+\nu)}{a^2}, \quad \nabla_\theta^2 = \frac{1}{a^2 \sin \theta} \frac{\partial}{\partial \theta} \sin \theta \frac{\partial}{\partial \theta}, \quad (35.f)$$

where  $E$  is the Young's modulus,  $\nu$  the Poisson's ratio and  $\beta^2 = h^2 / 12a^2$ .

The displacement components  $u_r$  and  $u_\theta$  can be expanded in spherical harmonics

$$u_r = \sum_n W_n P_n(\cos \theta), \quad u_\theta = \sum_n V_n \sin \theta P'_n(\cos \theta), \quad (36)$$

and the sound fields in both regions are given by

$$p_1 = p_{inc} + \sum_n D_n h_n^{(2)}(k_1 r) P_n(\cos \theta), \quad k_1 = \omega / c_1 \quad (37.a)$$

$$p_2 = \sum_n T_n j_n(k_2 r) P_n(\cos \theta), \quad k_2 = \omega / c_2 \quad (37.b)$$

Inserting (36) into (35) together with the boundary conditions of continuity of normal displacement, the coefficients  $W_n$ ,  $V_n$ ,  $D_n$  and  $T_n$  can be determined.

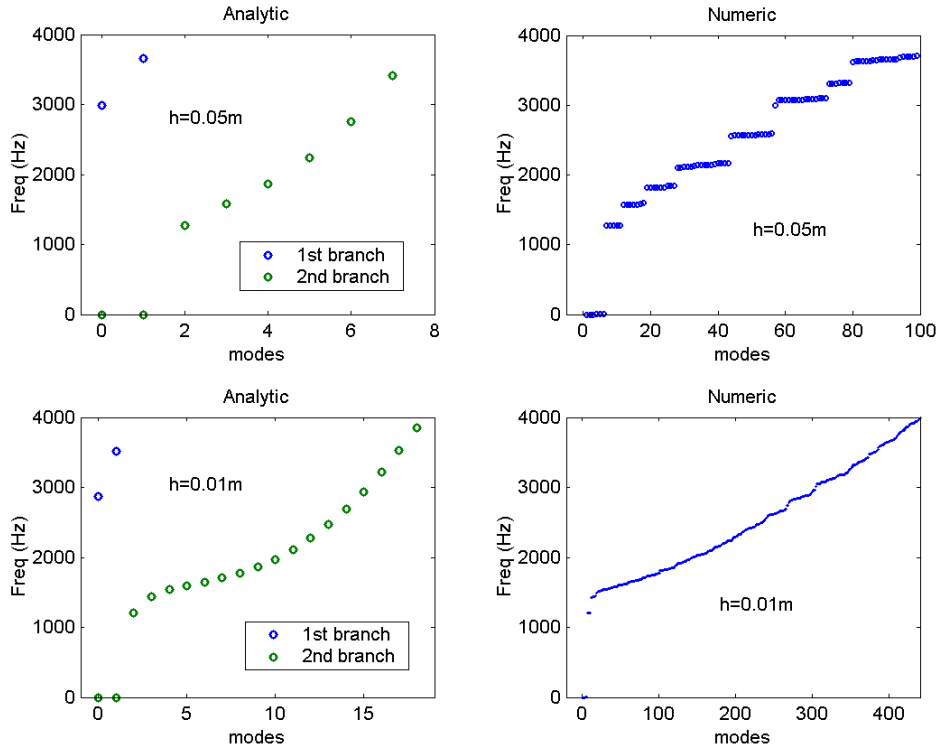


Fig. 7: Modes of the spherical shell

The analytic eigenfrequencies are given by the expression

$$\omega_n = \frac{c_p}{a\sqrt{2}} \sqrt{U_n^{(1)} + U_n^{(2)} \pm \sqrt{(U_n^{(1)} - U_n^{(2)})^2 + 4n(n+1)(U_n^{(3)})^2}} \quad (38)$$

with

$$U_n^{(1)} = 2(1 + \nu) + \beta^2 n(n+1)(n(n+1) + \nu - 1) \quad , \quad U_n^{(2)} = (1 + \beta^2)(n(n+1) + \nu - 1) \quad ,$$

$$U_n^{(3)} = \beta^2 (n(n+1) + \nu - 1) + 1 + \nu \quad , \quad c_p = \frac{E}{\rho(1 - \nu^2)} \quad .$$

Eq. (38) has two branches, one for the + sign and the other for the - sign, which indicates that if the number of terms of the expansions (36) is  $N$ , the number of eigenmodes considered is  $2N$ . A comparison of the analytical modes calculated using (38) and the modes computed numerically is presented in Fig. 7 for two different values of  $h$ . The number of numerical modes is clearly a lot bigger than the analytical ones in part because all possible modes are computed (for the analytical case only axisymmetric modes are considered) and also the method to find the numerical modes provide solutions that differ in small quantities.

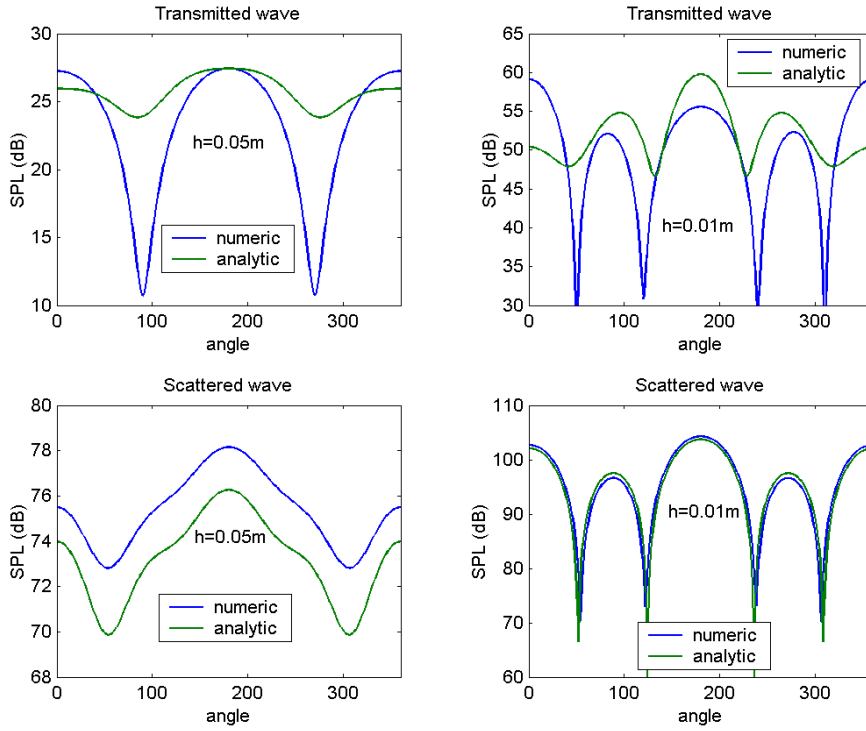


Fig. 8: Transmitted and scattered waves due to a spherical thin shell

The sound field is evaluated inside the sphere at a radius  $a/2$  and outside the sphere at a radius  $2a$ . A comparison of the results of the numerical approach and the analytical solution is shown in Fig. 8. The transmitted field shows similar form but the amplitude differs significantly from the analytical solution at some angles (upper curves), while the agreement of the scattered field is a lot better (lower curves). The agreement seems to improve when the thickness of the shell decreases. To explain this difference in accuracy we recall that the sound pressure at the outer surface of the sphere is a sum of incident and scattered wave, while the pressure at the inner surface is only the transmitted wave. Since the magnitude of the scattered and transmitted wave is smaller than the magnitude of the incident wave, the errors in the values of the scattered and transmitted waves have a bigger influence on the sound field inside the structure than outside, as is observed in Fig. 8.

## Summary

A numerical method to compute the sound transmission through slits and thin structures was presented. To determine the radiated sound, a direct BEM approach was considered. When there is a slit, continuity of pressure and normal velocity has to be imposed. When the thin structure is present, continuity of normal displacement is prescribed. By expanding the displacement of the structure into the eigenmodes, the system of equations can be reduced considerably. The method was tested using benchmark problems and analytical solutions. For slits and baffled plates the method works very well, for spherical shells some differences were found. The deviations may be possibly produced by the different approaches to obtain the eigenvalues and the occurrence of numerical errors due to the large difference in magnitude of incident and scattered waves.

## Acknowledgements

This work was supported by the German Research Foundation (DFG) within the Research Project "The acoustical transmission problem for plate-like structures (ATMOS)".

## REFERENCES

- [1] N. Gorenflo, A new explicit solution method for the diffraction through a slit - Part 2, *Zeitschrift für angewandte Mathematik und Physik ZAMP*, **volume 58**, 16-36, 2007.
- [2] R. Woodcock, J. Nicolas, A generalized model for predicting the sound transmission properties of generally orthotropic plates with arbitrary boundary conditions, *J. Acoust. Soc. Am.*, **volume 97 (2)**, 1099-1112, 1995.
- [3] S. Amini, P.J. Harris, D.T. Wilton, *Coupled Boundary and Finite Element Methods for the Solution of the Dynamic Fluid-Structure Interaction Problem*, editors C.A. Brebbia and S.A. Orszag, Springer-Verlag, 1992.
- [4] W. Bogusz, Z Dzygadlo, D. Rogula, K. Sobczyk, L. Solarz, *Vibration and Waves, Part A: Vibrations*, Elsevier, 1992.